The pH dependence of Am(III) complexation with acetate: an EXAFS study

Daniel R. Fröhlich,[a,b]* **Andrej Skerencak-Frech,**[b] **Nicole Bauer,**[a,b] **André Rossberg**[c] **and Petra J. Panak**[a,b]

[a]Physikalisch-Chemisches Institut, Ruprecht-Karls-Universität Heidelberg, Im Neuenheimer Feld 253, 69120 Heidelberg, Germany, [b]Institut für Nukleare Entsorgung, Karlsruher Institut für Technologie, PO Box 3640, 76021 Karlsruhe, Germany, and [c]Institut für Resourcenökologie, Helmholtz-Zentrum Dresden-Rossendorf, PO 510119, 01314 Dresden, Germany.
*E-mail: daniel.froehlich@partner.kit.edu

The complexation of acetate with Am(III) is studied as a function of the pH (1–6) by extended X-ray absorption fine-structure (EXAFS) spectroscopy. The molecular structure of the Am(III)–acetate complexes (coordination numbers, oxygen and carbon distances) is determined from the raw k^3-weighted Am L_{III}-edge EXAFS spectra. The results show a continuous shift of Am(III) speciation with increasing pH value towards the complexed species. Furthermore, it is verified that acetate coordinates in a bidentate coordination mode to Am(III) (Am—C distance: 2.82 ± 0.03 Å). The EXAFS data are analyzed by iterative transformation factor analysis to further verify the chemical speciation, which is calculated on the basis of thermodynamic constants, and the used structural model. The experimental results are in very good agreement with the thermodynamic modelling.

Keywords: americium; acetate; coordination chemistry; EXAFS; ITFA.

1. Introduction

The aqueous speciation and chemical behaviour of actinides in environmental systems is determined by different geochemical processes, *e.g.* sorption, diffusion, solubility and complexation with (in)organic ligands. These processes depend on a variety of parameters (*e.g.* pH, partial pressure of CO_2, ionic strength, temperature, *etc.*). In the context of nuclear waste storage in clay formations, which are taken into account as possible host rock formations in several European countries [*e.g.* Belgium (ONDRAF/NIRAS, 2001), France (OECD, 2006), Germany (Hoth *et al.*, 2007), Switzerland (NAGRA, 2002)], natural organic matter is of particular interest with respect to actinide speciation and migration processes. These natural-occurring clay organic compounds consist of complex macromolecules as well as simple carboxylic acids (*e.g.* formate, acetate, propionate, *etc.*) (Courdouan *et al.*, 2007*a*,*b*). Studies on the characterization of dissolved organic compounds in the pore waters of different natural clays showed that these small organic ligands make up large fractions of the total dissolved organic content (up to 88%) (Courdouan *et al.*, 2007*a*,*b*). Acetate is one of the major compounds with concentrations in the millimolar range and is therefore of particular interest.

In the near-field of a nuclear waste repository in a deep geological formation, reducing conditions are likely to prevail (for example, due to corrosion of the steel canisters). Furthermore, speciation calculations for anaerobic conditions

in an Opalinus Clay formation, which is investigated as possible host rock in Switzerland, indicate that +III will be the predominant oxidation state of plutonium and americium (Bradbury & Baeyens, 2003). Owing to their long half-lives, these trivalent actinides will contribute significantly to the long-term radiotoxicity of the nuclear waste material and are thus of high relevance for a reliable safety assessment of a potential storage site.

The aim of the present study is to investigate the complexation of Am(III) with acetate in aqueous solution by extended X-ray absorption fine-structure (EXAFS) spectroscopy. The interaction is studied systematically by varying the pH value between 1 and 6. In this pH range the formation of complexes with OH^- and CO_3^{2-} or ternary species can be excluded. Structural data of the formed Am(III)–acetate species (coordination numbers, Am—O and Am—C distances) are obtained from the raw Am L_{III}-edge EXAFS spectra. Furthermore, the fit results are verified by iterative transformation factor analysis (ITFA) and the spectroscopically determined coordination numbers are compared with those determined by thermodynamic speciation calculation.

In the literature a number of EXAFS studies on the interaction of acetate with different actinides can be found [Th(IV) (Rao *et al.*, 2004), U(VI) (Bailey *et al.*, 2004; Jiang *et al.*, 2002; Lucks *et al.*, 2012), Np(IV) (Takao *et al.*, 2012), Np(V,VI) (Takao *et al.*, 2009)]. However, no EXAFS data on the

research papers

complexation of Am(III) or other trivalent actinides with acetate are available. Thus, the present work will add to a molecular-level understanding of the solution chemistry of trivalent actinides with carboxylic ligands. Furthermore, Am(III) data can also be used to describe the geochemical behaviour of Pu(III).

2. Experimental section

2.1. Sample preparation

Six samples were prepared in total. The total concentration of acetate in the samples was fixed at $[Ac^-]_{tot} = 0.2\ M$ by dissolution of solid NaAc (Merck, suprapure) in water (Millipore grade). The concentration of Am(III) was fixed at $[Am(III)]_{tot} = 10^{-3}\ M$ by adding a defined quantity of an Am(III) stock solution ($[^{243}Am] = 30\ MBq\ ml^{-1}$, $[^{241}Am] = 17\ MBq\ ml^{-1}$). The concentration of Am(III) was checked by γ spectrometry and ICP-MS analysis. The pH of the respective samples was set to pH = 1.04, 1.91, 3.41, 3.97, 4.89 and 5.90 by adding defined quantities of 2 M HCl (Merck, suprapure) or freshly prepared 2 M NaOH (Merck, Titrisol), respectively. The pH was measured by a combination pH electrode (Ross, ORION), which was freshly calibrated against dilute standard buffer solutions (Merck, pH 3, 6, 10).

2.2. EXAFS spectroscopy

Am L_{III}-edge EXAFS spectra of all samples were measured in fluorescence mode using a 13-element Ge detector at the Rossendorf beamline (ROBL, BM20) at the European Synchrotron Radiation Facility (ESRF, Grenoble, France). The detector was positioned at an angle of 90° relative to the incoming beam. For energy calibration a zirconium foil was measured simultaneously in transmission mode. A detailed description of the beamline is given elsewhere (Matz *et al.*, 1999). The whole data processing, including dead-time correction, energy calibration, averaging, extraction of the EXAFS signal and fitting, was performed using the *EXAFSPAK* software package (George & Pickering, 2000). In all cases, the ionization energy (E_0) was set to 18515 eV. Theoretical scattering phases and amplitudes were calculated with *FEFF8.20* (Ankudinov *et al.*, 2002) using the crystal structure of Eu(CH$_3$COO)$_2$ × 0.5H$_2$O (Starynowicz, 1998) as model crystal structure (Eu replaced by Am). The potentials were calculated using the self-consistent field approach. In all cases the best theoretical model was fit to the raw k^3-weighted EXAFS spectra using the Marquardt algorithm. The amplitude reduction factor S_0^2 was held constant at 0.9.

2.3. Speciation calculations

The thermodynamic speciation calculation was performed using the software package *Visual MINTEQ* (Version 3.0) (Gustafsson, 2012) in order to determine the aqueous speciation of 1 mM Am(III) in a 0.2 M NaAc solution as a function of the pH at ambient air conditions (pCO$_2$ = 0.00038 atm). Ionic strength corrections are taken into account using the Davies equation (Davies, 1938). The ther-

Table 1
Standard state stability constants of the different complexation reactions used for speciation calculations. All constants originate from the NIST databases 46.6 and 46.7 or from Plummer & Busenberg (1982).

Reaction	Log K^0
$Am^{3+} + H_2O \rightleftharpoons AmOH^{2+} + H^+$	−6.497
$Am^{3+} + 2H_2O \rightleftharpoons AmOH_2^+ + 2H^+$	−14.094
$Am^{3+} + 3H_2O \rightleftharpoons AmOH_3\ (aq) + 3H^+$	−25.691
$Am^{3+} + CO_3^{2-} \rightleftharpoons AmCO_3^+$	7.8
$Am^{3+} + 2CO_3^{2-} \rightleftharpoons Am(CO_3)_2^-$	12.3
$Am^{3+} + Ac^- \rightleftharpoons AmAc^{2+}$	2.6
$Am^{3+} + 2Ac^- \rightleftharpoons AmAc_2^+$	4.39
$Am^{3+} + 3Ac^- \rightleftharpoons AmAc_3\ (aq)$	4.99
$H^+ + Ac^- \rightleftharpoons HAc\ (aq)$	4.757
$Na^+ + Ac^- \rightleftharpoons NaAc\ (aq)$	−0.12
$Na^+ + OH^- \rightleftharpoons NaOH\ (aq)$	−13.897
$H_2O \rightleftharpoons H^+ + OH^-$	−13.997
$H^+ + CO_3^{2-} \rightleftharpoons HCO_3^-$	10.329
$2H^+ + CO_3^{2-} \rightleftharpoons H_2CO_3\ (aq)$	16.681

modynamic stability constants of the considered complexation reactions are given in Table 1. The constants of the database of *Visual MINTEQ* are taken from NIST databases 46.6 and 46.7 or from Plummer & Busenberg (1982).

2.4. ITFA

All EXAFS spectra were analyzed by ITFA (Rossberg *et al.*, 2003). This procedure involves three steps: the principal component analysis, the VARIMAX procedure, and the iterative target test. The VARIMAX procedure yields factor loadings that correlate to the relative concentrations of the pure components in the spectra. The iterative target test calculates the relative concentrations of the pure components. However, for this step constraints have to be defined (see §3.3). Once the relative concentrations for each spectrum are determined by the iterative target test, the spectra of the pure components are calculated. More information on the application of ITFA to the complexation of actinides with organic ligands as well as a detailed description of the different analysis steps can be found elsewhere (Lucks *et al.*, 2012). In the present work, ITFA is used to deconvolute the experimental EXAFS spectra by using the spectra of two components, *i.e.* Am(III) with a complete water shell and a hypothetical Am(III) species with a complete ligand surrounding where all oxygen atoms in the first coordination sphere belong to carboxylic functions of acetate (see also §3.3). The resulting component spectra are extracted and fitted with *EXAFSPAK* as described above to validate the used structural model. Furthermore, the speciation resulting from the ITFA is used to calculate the average coordination numbers for each sample and the results are compared with the results of the EXAFS fits and the thermodynamic speciation calculation.

3. Results

3.1. EXAFS

Fig. 1 shows the experimental raw k^3-weighted Am L_{III}-edge EXAFS spectra of samples 1–6 together with the

Table 2
Fit parameters of the raw k^3-weighted Am L_{III}-edge EXAFS spectra shown in Fig. 1.

Sample		1	2	3	4	5	6
pH		1.04	1.91	3.41	3.97	4.89	5.90
O	N	10.1 (3)	10.1 (4)	10.4 (5)	10.2 (4)	10.7 (5)	10.4 (5)
	R (Å)	2.47 (1)	2.47 (1)	2.48 (1)	2.49 (1)	2.49 (1)	2.49 (1)
	σ^2 (Å²)	0.009 (1)	0.009 (1)	0.009 (1)	0.009 (1)	0.010 (1)	0.009 (1)
$C_{carboxyl}$†	N	–	–	0.4 (4)	1.0 (3)	1.6 (0.4)	2.0 (4)
	R (Å)	–	–	2.78 (7)	2.81 (3)	2.83 (2)	2.84 (1)
C_{distal}‡	R (Å)	–	–	4.39 (9)	4.41 (4)	4.41 (3)	4.41 (2)
ΔE_0 (eV)		−2.0 (3)	−2.1 (3)	−1.6 (4)	−1.0 (3)	−1.0 (4)	−0.3 (4)
Reduced error without C shells		0.192	0.217	0.185	0.177	0.219	0.234
Reduced error with C shells		–	–	0.183	0.174	0.213	0.214
k-range (Å)$^{-1}$		1.8–10.8	1.8–10.8	1.8–10.8	1.7–10.8	1.7–10.8	1.8–10.8

† σ^2 held constant at 0.003 Å². ‡ N of C_{distal} linked to N of $C_{carboxyl}$, σ^2 held constant at 0.006 Å², S_0^2 was set to 0.9 in all cases, uncertainties of each value obtained from the *EXAFSPAK* fit are given in parentheses. The absolute errors are: $N \pm 20\%$, $R \pm 0.02$ Å (Li *et al.*, 1995).

corresponding Fourier transforms (FT) and the fit curves. Comparing the spectra in Fig. 1, only slight changes with pH are obtained, *e.g.* a small peak at high distance in the FT which appears at high pH values. The resulting fit parameters are given in Table 2. During the fitting procedure the Debye–Waller factors related to the carboxylic and distal carbon neighbours are held constant at 0.003 and 0.006 Å², respectively. The coordination number (N) of the distal carbon atom is linked to N of the carboxylic carbon. In all cases about ten oxygen neighbours at a distance between 2.47 and 2.49 Å are found in the first coordination sphere. This value is in good agreement with coordination numbers and oxygen distances of Am(III) [$N = 8.9$–10.3, $R = 2.48$–2.51 Å (Allen *et al.*, 2000)] and other trivalent actinides in aqueous solution [$N = 9.0$–10.2, $R = 2.44$–2.52 Å (Allen *et al.*, 2000; Brendebach *et al.*, 2009)] reported in the literature. Whereas the spectra at pH = 1–2 are well described by an oxygen shell only, the spectra at higher pH values have been fitted with and without considering the
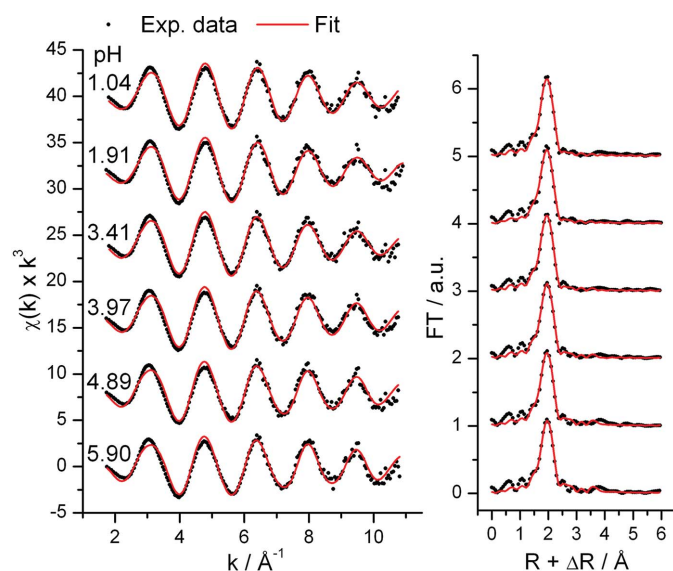
carboxylic and distal carbon atoms. The reduced error of the fit improves slightly for samples 3–5 when the carbon shells are taken into account (see Table 2), confirming the prevalence of carboxylic coordination with increasing pH. In the case of the spectrum at highest pH (5.9), the improvement of the reduced error is even more pronounced. The number of carbon neighbours increases continuously from 0.4 at pH = 3.4 to 2.0 at pH = 5.9. For all samples, comparable distances are obtained for the distal carbon atoms (4.39–4.41 Å). Whereas the Am—C_{distal} distance remains cons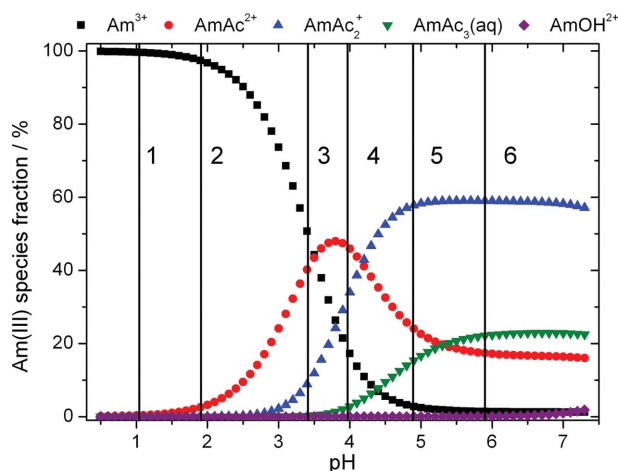tant, the Am—$C_{carboxyl}$ distance (2.78–2.84 Å) shows a slight but continuous increase with increasing number of ligands.

These values are compared with EXAFS data of acetate complexes of U(VI) [$C_{carboxyl}$: 2.87–2.91 Å (Bailey *et al.*, 2004; Jiang *et al.*, 2002; Lucks *et al.*, 2012), C_{distal}: 4.36 Å (Lucks *et al.*, 2012)], Np(V) [$C_{carboxyl}$: 2.91–2.93 Å (Takao *et al.*, 2009)] and Np(VI) [$C_{carboxyl}$: 2.87 Å, C_{distal}: 4.38 Å (Takao *et al.*, 2009)]. These values are in good agreement with the results in the present work. Slight differences are addressed to the structural differences of the formed complexes as U(VI) and Np(V/VI) form UO_2^{2+} and $NpO_2^{+/2+}$ ions, respectively. Furthermore, it can be concluded that Am(III)–acetate binding occurs in a bidentate end-on coordination. Monodentate binding would result in significantly longer Am—$C_{carboxyl}$ distances.

3.2. Speciation calculations

The experimental data were compared with the thermodynamic calculation which was performed with *Visual MINTEQ* (Version 3.0) as stated above. The speciation of Am(III) as a function of the pH value in 0.2 NaAc solution is shown in Fig. 2. The vertical lines indicate the pH values of the EXAFS samples. The Am(III)–aquo ion is the dominating species up to pH $\simeq$ 3. The formation of AmAc^{2+} starts at pH $\simeq$ 2, reaching its maximum ($\sim$50%) at about pH 3.7. The 1:2 and 1:3 species of Am(III) with acetate are formed above pH = 3 and pH = 4, respectively. The fractions of these Am(III)–acetate species increase continuously up to pH $\simeq$ 5.5. Between pH $\simeq$ 5.5 and 7, the Am(III) speciation remains almost constant with $\sim$17% AmAc^{2+}, $\sim$59% AmAc$_2^+$ and $\sim$23% AmAc$_3$ (aq). At higher pH, the amount of Am(III)–acetate species decreases due to formation of hydroxo- and carbonate species. As shown in Fig. 2, the formation of Am(III)–hydroxo or Am(III)–carbonate species in the pH range studied by EXAFS spectroscopy is negligible.

The calculated Am(III) speciation (Fig. 2) is used to determine the average coordination number with respect to acetate in each point. The calculated coordination number as a function of the pH value is compared with the values obtained from EXAFS fitting (see Fig. 3, top). The experimentally determined values are in very good agreement with the
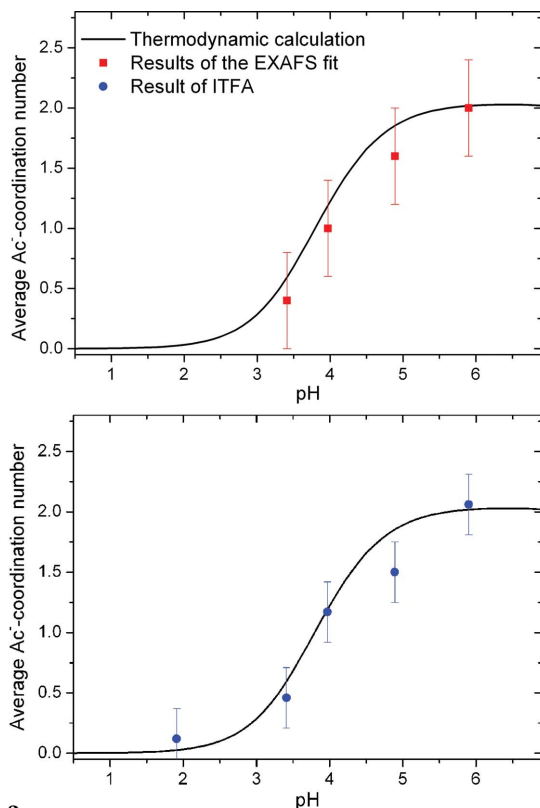

Figure 1
Left: raw k^3-weighted Am L_{III}-edge EXAFS spectra (black dots) of 1 mM Am(III) in 0.2 M NaAc solution as a function of the pH together with the best fit from *EXAFSPAK* (red lines). Right: Corresponding Fourier transforms.

Figure 2
Speciation of Am(III) in 0.2 M NaAc solution at ambient air conditions as a function of the pH value (species below 1% not shown). The vertical lines indicate the pH of the EXAFS samples 1–6 (see *Experimental section*).

coordination numbers calculated on the basis of thermodynamic data.

3.3. ITFA

ITFA is performed with the raw k^3-weighted Am L_{III}-edge EXAFS spectra. Unfortunately, only six experimental spectra do not exhibit the statistics necessary to deconvolute them with four species {Am(III)–aquo, $[AmAc_x]^{3-x}$ (x = 1–3)}.

Figure 3
Average coordination number with respect to acetate as a function of the pH value obtained from EXAFS (top) and ITFA (bottom) compared with the thermodynamic calculation.

Table 3
ITFA-determined fractions of the two components in the EXAFS pH series.

		Amount of component (%)	
Sample	pH	Component 1	Component 2
1	1.04	100†	0
2	1.91	98	2
3	3.41	91	9
4	3.97	78	22
5	4.89	71	29
6	5.90	60†	40

† Held constant during fit.

Following this approach, the resulting pure component spectra are too noisy to analyze them with *EXAFSPAK*. Thus, we deconvoluted the EXAFS spectra considering two distinct components completely coordinated either by H_2O or acetate (see also §2.4). As the fit of the EXAFS spectra provided a coordination number of ~10 in all cases (see Table 2), the spectrum of component 2 corresponds to a hypothetical Am(III) species coordinated by five acetate ligands. To obtain a quantitative result from the iterative target test some selected relative concentrations have to be fixed during the fit [details are described elsewhere (Rossberg *et al.*, 2003)]. In the case of two components, two relative concentrations have to be held constant. Thus, the fractions of component 1 are fixed to 100% for sample 1 and 60% for sample 6 as determined experimentally by EXAFS.

The resulting amounts of both species for each spectrum are given in Table 3. The amount of component 2 increases continuously with increasing pH due to the formation of Am(III)–acetate species. This speciation is used to calculate the average coordination numbers. Fig. 3 (bottom) shows the results compared with the thermodynamic calculation. As for the EXAFS spectroscopic results, a good agreement in the entire pH range studied is found.

The ITFA extracted component EXAFS spectra are fitted with *EXAFSPAK* following the same procedure as for the experimental spectra. The EXAFS spectra, the related FTs and the fit curves are shown in Fig. 4. The resulting fit parameters are given in Table 4. Component 1 is characterized by one shell of 10.4 oxygen atoms at 2.48 Å. In the case of component 2, the Am—O distance is slightly longer (2.52 Å) as it is expected for a quantitative complexation with bidentate binding carboxylic groups. The same trend was found for the complexation of U(VI) with acetate. There, the U—O distance increased continuously with increasing number of coordinating ligands from 2.40 (number of ligands = 0) to 2.47 Å (number of ligands = 3) (Lucks *et al.*, 2012). The coordination number of carbon atoms of component 2 equals 5.2 ± 0.5. This verifies the structural model which has been used for the EXAFS fitting. The carboxylic and distal carbon atoms are located at 2.87 and 4.44 Å, respectively. These values are slightly higher compared with the results of samples 1–6. However, this is in agreement with the slight continuous increase of the Am—$C_{carboxyl}$ distance with increasing number of ligands (compare Table 2).
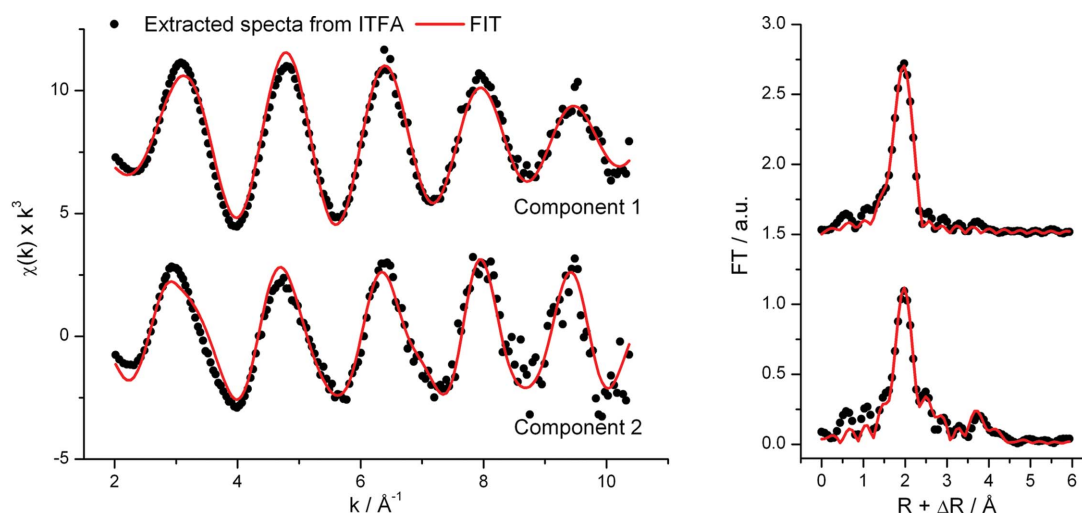
Figure 4
Left: k^3-weighted EXAFS spectra of the components 1 and 2 obtained from ITFA. Right: Corresponding Fourier transforms.

Table 4
Fit parameters of component 1 and 2 spectra obtained from ITFA (Fig. 4).

Component		1	2
O	N	10.4 (3)	10.2 (6)
	R	2.48 (1)	2.52 (1)
	σ^2	0.009 (1)	0.009 (1)
C†	N	–	5.2 (5)
	R	–	2.87 (1)
C_{dist}‡	R	–	4.44 (1)
ΔE_0		−1.7 (2)	1.2 (5)
Reduced error		0.133	0.361
k-range		2.0–10.4	2.0–10.4

† σ^2 held constant at 0.003 Å^2. ‡ N of C_{dist} linked to N of the $C_{carboxyl}$, σ^2 held constant at 0.006 Å^2, S_0^2 was set to 0.9 in all cases, uncertainties of each value obtained from the *EXAFSPAK* fit are given in parentheses. The absolute errors are: $N \pm 20\%$, $R \pm 0.02$ Å (Li *et al.*, 1995).

4. Summary

The present EXAFS study shows that the impact of acetate on Am(III) speciation increases continuously with increasing pH value in the studied pH range. The average coordination number with respect to acetate increases from 0 at pH = 1.0 to 2 at pH = 5.9. In all cases Am(III) is surrounded by about ten oxygen atoms in the first coordination sphere. The Am—O (2.47–2.49 Å), Am—$C_{carboxyl}$ (2.78–2.84 Å) and Am—C_{distal} (4.39–4.41 Å) distances agree within the range of error for all samples. Additionally, the Am—O and Am—$C_{carboxyl}$ distances increase slightly with increasing number of ligands. The determined structural parameters clearly show that acetate binding occurs in a bidentate end-on coordination.

ITFA has been applied to extract the component EXAFS spectra of the Am(III)–aquo ion (component 1) and Am(III) completely coordinated by acetate ligands (component 2). The structural data obtained for component 1 are in excellent agreement with the values of samples 1 (pH = 1.0) and 2 (pH = 1.9). For component 2, the Am(III)—O, Am—$C_{carboxyl}$ and Am—C_{distal} distances are 2.52 Å, 2,87 Å and 4.44 Å, respectively. These values are slightly higher compared with the parameters obtained from the experimental EXAFS data.

This is in agreement with the trend of increasing Am(III)—O and Am—$C_{carboxyl}$ distances with increasing number of ligands in this work and literature data for U(VI) (Lucks *et al.*, 2012). The average coordination numbers determined by ITFA and experiment are in line with the predicted coordination numbers obtained from thermodynamic calculations.

The structural data of Am(III)–acetate complexation obtained in this work will help to improve the description and molecular-level understanding of the environmental aqueous geochemistry of trivalent actinides.

References

Allen, P. G., Bucher, J. J., Shuh, D. K., Edelstein, N. M. & Craig, I. (2000). *Inorg. Chem.* **39**, 595–601.
Ankudinov, A. L., Bouldin, C. E., Rehr, J. J., Sims, J. & Hung, H. (2002). *Phys. Rev. B*, **65**, 104107.
Bailey, E. H., Mosselmans, J. F. W. & Schofield, P. F. (2004). *Geochim. Cosmochim. Acta*, **68**, 1711–1722.
Bradbury, M. H. & Baeyens, B. (2003). PSI Technical Report 03–08. Paul Scherrer Institut, Villigen, Switzerland.
Brendebach, B., Banik, N. L., Marquardt, C. M., Rothe, J., Denecke, M. A. & Geckeis, H. (2009). *Radiochim. Acta*, **97**, 701–708.
Courdouan, A., Christl, I., Meylan, S., Wersin, P. & Kretzschmar, R. (2007a). *Appl. Geochem.* **22**, 1537–1548.
Courdouan, A., Christl, I., Meylan, S., Wersin, P. & Kretzschmar, R. (2007b). *Appl. Geochem.* **22**, 2926–2939.
Davies, C. W. (1938). *J. Chem. Soc.* pp. 2093–2098.
George, G. N. & Pickering, I. J. (2000). *EXAFSPAK: A suite of computer programs for analysis of X-ray absorption spectra.* Stanford Synchrotron Radiation Laboratory, Stanford, USA.

Gustafsson, J. P. (2012). *Geochemical equilibrium speciation model Visual MINTEQ* Version 3.0. KTH Royal Institute of Technology, Department of Land and Water Resources Engineering, Stockholm, Sweden.

Hoth, P., Wirth, H., Reinhold, K., Bräuer, V., Krull, P. & Feldrappe, H. (2007). *Endlagerung radioaktiver Abfälle in tiefen geologischen Formationen Deutschlands–Untersuchung und Bewertung von Tongesteinsformationen.* BGR Bundesanstalt für Geowissenschaften und Rohstoffe, Hannover, Germany.

Jiang, J., Rao, L., Di Bernardo, P., Zanonato, P. L. & Bismondo, A. (2002). *J. Chem. Soc. Dalton Trans.* **8**, 1832–1838.

Li, G. G., Bridges, F. & Booth, C. H. (1995). *Phys. Rev. B*, **52**, 6332–6348.

Lucks, C., Rossberg, A., Tsushima, S., Foerstendorf, H., Scheinost, A. C. & Bernhard, G. (2012). *Inorg. Chem.* **51**, 12288–12300.

Matz, W., Schell, N., Bernhard, G., Prokert, F., Reich, T., Claußner, J., Oehme, W., Schlenk, R., Dienel, S., Funke, H., Eichhorn, F., Betzl, M., Pröhl, D., Strauch, U., Hüttig, G., Krug, H., Neumann, W., Brendler, V., Reichel, P., Denecke, M. A. & Nitsche, H. (1999). *J. Synchrotron Rad.* **6**, 1076–1085.

NAGRA (2002). *Projekt Opalinuston–Synthese der geowissenschaftlichen Untersuchungsergebnisse, Entsorgungsnachweis für abgebrannte Brennelemente, verglaste hochaktive sowie langlebige mittelaktive Abfälle.* Technical Report NTB 02–03. NAGRA Nationale Genossenschaft für die Lagerung radioaktiver Abfälle, Wettingen, Switzerland.

OECD (2006). *Safety of geological disposal of high-level and long-lived radioactive waste in France-An international peer review of the 'Dossier 2005 Argile' concerning disposal in the Callovo-Oxfordian formation.* NEA No. 6178. OECD Organisation for economic co-operation and development.

ONDRAF/NIRAS (2001). *SAFIR 2: Safety Assessment and Feasibility Interim Report.* NIROND-2001–06 E. ONDRAF/NIRAS, Brussels, Belgium.

Plummer, L. N. & Busenberg, E. (1982). *Geochim. Cosmochim. Acta*, **46**, 1011–1040.

Rao, L., Zhang, Z., Zanonato, P. L., Di Bernardo, P., Bismondo, A. & Clark, S. B. (2004). *Dalton Trans.* pp. 2867–2872.

Rossberg, A., Reich, T. & Bernhard, G. (2003). *Anal. Bioanal. Chem.* **376**, 631–638.

Starynowicz, P. (1998). *J. Alloys Compd.* **268**, 47–49.

Takao, K., Takao, S., Scheinost, A. C., Bernhard, G. & Hennig, C. (2009). *Inorg. Chem.* **48**, 8803–8810.

Takao, K., Takao, S., Scheinost, A. C., Bernhard, G. & Hennig, C. (2012). *Inorg. Chem.* **51**, 1336–1344.